Steel and Composite Structures, *Vol. 29, No. 4 (2018) 509-526*
DOI: https://doi.org/10.12989/scs.2018.29.4.509

Direct strength method for high strength steel welded section columns

Jong Yoon Choi [1a] and Young Bong Kwon [*2]

[1] *Structural Division, Dae Han Concultants Co., Ltd., Seoul, Republic of Korea*
[2] *Department of Civil Engineering, Yeungnam University, Gyongsan, Republic of Korea*

(*Received April 9, 2018, Revised October 18, 2018, Accepted October 29, 2018*)

Abstract. The direct strength method adopted by the AISI Standard and AS/NZS 4600 is an advanced design method meant to substitute the effective width method for the design of cold-formed steel structural members accounting for local instability of thin plate elements. It was proven that the design strength formula for the direct strength method could predict the ultimate strength of medium strength steel welded section compressive and flexural members with local buckling reasonably. This paper focuses on the modification of the direct strength formula for the application to high strength and high performance steel welded section columns which have the nominal yield stress higher than 460 MPa and undergo local buckling, overall buckling or their interaction. The resistance of high strength steel welded H and Box section columns calculated by the proposed direct strength formulae were validated by comparison with various compression test results, FE results, and predictions by existing specifications.

Keywords: Direct Strength Method; high strength steel; high performance steel; welded section columns; ultimate strength; buckling interaction

1. Introduction

General high strength steels manufactured by the thermos mechanical control process have nominal yield stresses which are higher than approximately 460 MPa. The ultimate strength and structural behavior of high strength steel columns were studied by many researchers for the practical use since 1980 (Usami and Fukumoto 1982, 1984, Rasmussen and Hancock 1992,1995, Ban *et al*. 2012, Li *et al*. 2016, Gao *et al*. 2009).

In addition to high strength, high strength steels have several advantages such as weldability, increased fatigue strength and comparatively smaller magnitude of residual stress than mild steel. High performance steel has been developed to retain those advantages and in addition, one or more of aseismic capacity, weather proof and so on. Since high strength is one of major aspects of high performance steel, the term of high strength steel means both high strength steel and high performance steel from here. Those advantages facilitate the increase of use of slender or noncompact plate elements for high performance and high strength steel structural members of large-scale buildings and bridges.

Welded steel compression members composed of slender or noncompact plate elements may normally undergo buckling interaction between local and global modes (Degée *et al*. 2008, Davis and Hancock 1986, Akrami and Erfani 2015, Park and Yoo 2013). If a column had a smaller local buckling stress than the global buckling, local and global buckling interaction may occur due to the post-buckling strength in local mode. With a considerable amount of post-local-buckling strength reserve, the interaction of buckling modes has a serious effect on the structural performance and ultimate strength of steel members significantly. The interaction between buckling modes generally deteriorates the overall member strength. The negative effects of buckling interactions should be considered in making a prediction of the ultimate strength of structural members.

For large scale buildings and bridges, seismic retrofitting and progressive collapse which may be incurred by buckling of structural members as well as failure of connections became very important research topics recently. The buckling-restrained brace is one of efficient retrofitting members for tall buildings which need large plastic deformation capacity and ductility under intensive compressive loading. Gheidi *et al*. (2011) studied the effect of various filler materials on local and global behavior of buckling-restrained braces not to allow buckling or strength deterioration and Mirtaheri *et al*. (2017) investigated local and global buckling condition of buckling-restrained braces without filler material. Mirtaheri and Zoghi (2016), Miyachi *et al*. (2012), Paik and Kim (2008) and Kenyon *et al*. (2018) studied the progressive collapse of steel framed structures and structural members.

The conventional effective width method (EWM) and direct strength method (DSM) are two tools that take account of the interaction of local and overall buckling in current design specifications. Recently AISC Specifications (AISC 2016) adopted new design procedures for column members to take into account the interaction of local and overall buckling. The procedures are more convenient to

∗Corresponding author, Professor,
E-mail: ybkwon@ynu.ac.kr
[a] Design Engineer, E-mail: sugi9@daecon.co.kr

http://www.techno-press.org/?journal=scs&subpage=6
ISSN: 1229-9367 (Print), 1598-6233 (Online)

use than previous one, which use an effective area concept instead of Q-factor design method which has been used until 2015.

The direct strength method was proposed by Schafer and Pekoz (1998) and extended by various researchers (Pham and Hancock 2012, Young *et al*. 2013, Martins *et al*. 2016). It was first adopted by AISI specifications in 2004 for the design of cold-formed steel members. The method was also adopted by the Australian/New Zealand Cold-Formed Steel Structures Standard (AS/NZS 4600) in 2005. However, the application of DSM to welded and hot rolled steel sections has not been studied widely since the buckling interaction is less severe in welded sections than in cold-formed steel sections. Kwon *et al*. (Kwon *et al*. 2007, Kwon and Seo 2013) executed compression tests for mild steel C, H and Box section columns. The proposed strength formulae for the DSM were based on the mild strength steel welded section columns. The DSM for mild steel welded section structural members was reviewed recently (Kwon 2014). High strength and high performance steel have different stress versus strain relation from the mild steel, and distribution and magnitude of residual stress are also significantly different. Therefore, the reliability of the proposed design strength formulae should be investigated for high strength and high performance steel structural members to ensure the safety of structures made of them.

This paper focuses on the application of DSM to high strength steel column members with local and global buckling interaction. Validated FE analyses for high strength steel columns were performed, and the column strength equations for the DSM were compared with test results in literature and FE results. A reliability study was also conducted for proposed DSM.

The proposed direct strength method can be chosen as an alternative design method in the current design specifications for the design of high strength steel welded section columns with local buckling, overall buckling or their interaction as the DSM has been adopted by the AISI specifications and AS/NZS 4600 for the design of the cold-formed steel structural members.

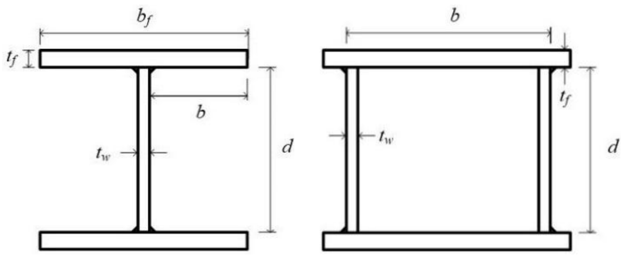

(a) H-section (b) Box-section

Fig. 1 Cross section of column members

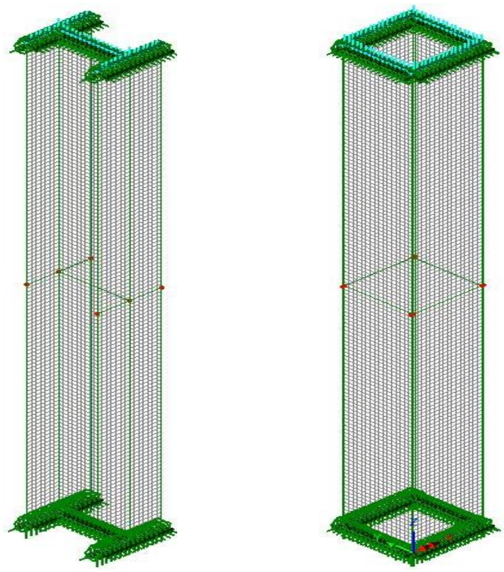

Fig. 2 FE models for H and Box section columns

2. Finite element modeling and verification

2.1 Model description and validation

An elastic buckling analysis of typical H and Box section columns shown in Figs. 1(a) and (b) was done to validate the FE model. In the FE analysis, the boundary condition of the unloaded bottom of the columns was assumed to be a hinged support in both direction, and the loaded end is assumed to be a roller support in vertical direction. The QTS4 4-node quadrilateral shell element in LUSAS software (FEA Co., Ltd. 2012) was chosen to execute linear elastic buckling analysis of columns. The FE models for H and Box section columns shown in Fig. 2 were taken to examine the convergence rate of the column buckling stress according to the mesh size of elements. A uniform mesh size was used over the whole column length. A uniformly distributed load was applied to the cross section at the top end of column, and an equal displacement constraint was applied at loaded end of the column instead of including end bearing plates in the FE model for comparison with the test results.

Figs. 3(a) and (b) show the relative errors for various meshes in the elastic buckling stress obtained with a mesh size 10 mm × 10 mm for H and Box section columns, respectively. The models with a mesh size 100 mm × 100 mm start to show somewhat reliable buckling stress in comparison with 10 mm × 10 mm mesh size results. The models with a mesh size of 30 mm × 30 mm produced reliable buckling stress with less than 2.0% variation of the relative error. Therefore, this 30 mm × 30 mm mesh was considered as the maximum mesh size required in further FE analyses of high performance steel columns.

2.2 Mechanical properties of high-performance steel

The stress versus strain curve of high performance and high strength steel is generally different from that of mild steel, which shows a clear yield plateau. High performance steel produced by a thermo-mechanical control process instead shows rounded curves from the proportional limit through the yield stress to the ultimate tensile stress in the stress versus strain relations. Therefore, the 0.2% offset stress is generally considered as the yield stress for high

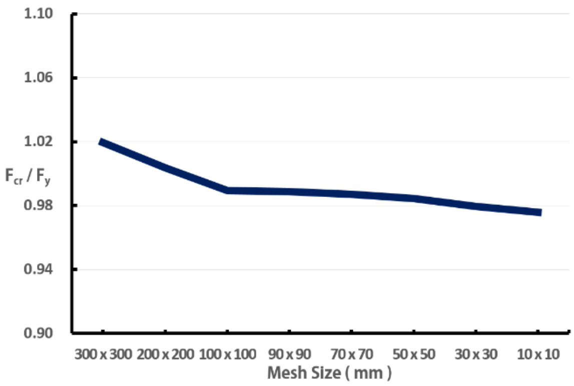

(a) H section column

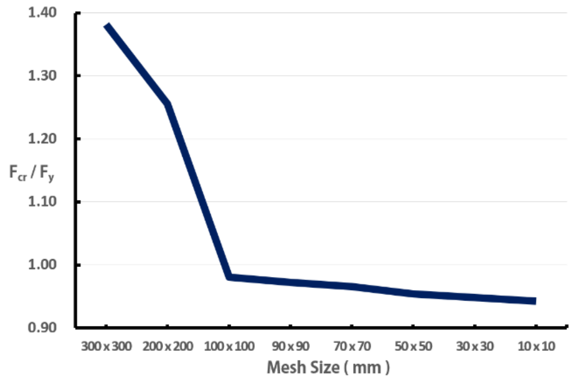

(b) Box section column

Fig. 3 Convergence study for mesh size

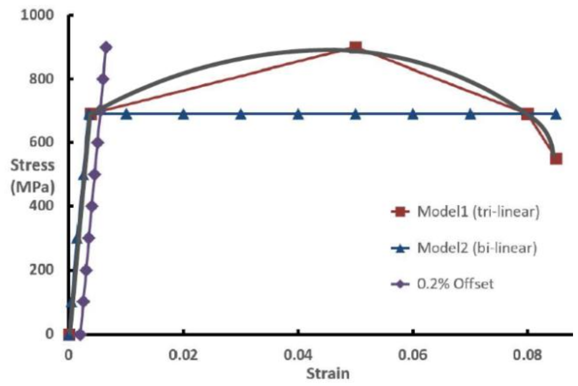

Fig. 4 Stress versus strain curves for high performance steel (HPA800)

performance steel in Korea, as shown in Fig. 4. The elongation of high strength steel is slightly smaller than that of mild steel, which means the ductility of the structural members is lower.

Fig. 4 shows two material models for the stress-strain relations of high performance steel. Material model 1 is a tri-linear curve that accounts for plastic strain hardening and assumes an initially isotropic yield surface based on the von Mises criterion and isotropic hardening. Material model 2 is an elastic-perfectly plastic stress-strain (bi-linear) relation that neglects strain-hardening, which is generally accepted for mild steel members. An elastic-perfectly plastic relation may be used for high strength steel as well as mild steel members. However, the different stress-strain models may cause significantly different structural behavior for compression members and therefore the effects should be checked.

Figs. 5(a) and (b) illustrate curves of axial load versus shortening obtained by FE analysis of typical H and Box sections with the two material models in Fig. 4. The yield and tensile stresses are 760 MPa and 890 MPa, which are higher than the nominal yield stress of 690 MPa and tensile stress of 800 MPa, respectively. The dimensions of H sections are b_f = 240 mm, t_f = 15 mm, d = 450 mm, and t_w = 15 mm for section A and b_f = 220 mm, t_f = 15 mm, d = 310 mm, and t_w = 15 mm for section B. The FE analysis results show that there is little difference between the results obtained with different models up to the peak load for both sections. However, a slight drop is observed after the peak load for section B with material model 1. The strain at the peak load ranges from 0.003 to 0.004 and is smaller than the yield strain of 0.0058, which was computed from the 0.2% offset yield stress and assuming that the yield stress is 760 MPa and Young's modulus is 2.0×10^5 MPa.

In tensile coupon tests, Kim *et al*. (2014) measured the average yield strain to be 0.38%, at which Young's modulus was slightly higher than 2.0×10^5 MPa. The effects of strain hardening on the maximum load of columns are negligible because the strain at maximum load is smaller than the yield strain. However, it slightly affects the post-peak load

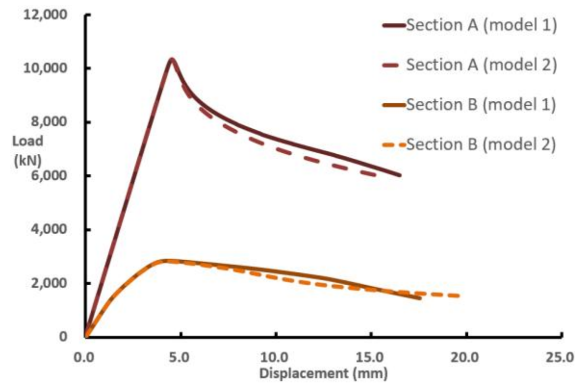

(a) Column length = 1200 mm

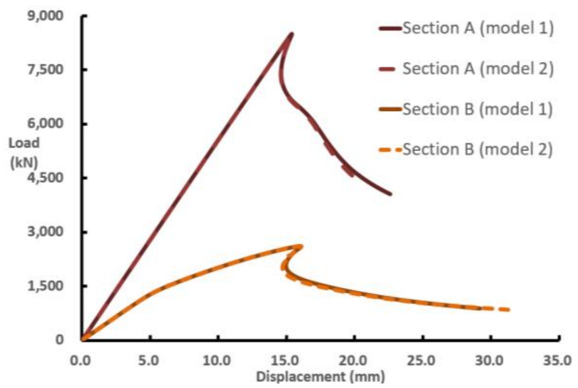

(b) Column length = 5000 mm

Fig. 5 Axial load versus shortening curves for high performance steel columns (section A: H-450-240-15-15, section B: H-310-220-15-15) behavior for short columns. Thus, both material models can be used in the nonlinear FE analysis of high performance steel section columns.

3. Finite element tests

3.1 General

Material and geometrical nonlinear analyses of test results from the literature were conducted using LUSAS software to verify the FE analysis results for the ultimate strength. The QTS4 4-node shell element with mesh size of 20 mm × 20 mm was used to numerically model H and Box section columns. The similar boundary conditions to the compression tests were provided. Hinged boundary condition was assumed at the unloaded bottom end and the loaded end was assumed to be a roller which is free to rotate about *x*- and *y*-axis and to move in z-direction for the application of a vertical load. The top column end was compressed in the vertical direction with uniform displacement control technique to acquire similar effects of a thick end bearing plate of the column in the compression test. The average test yield stress was used in the analysis, which was generally higher than the nominal yield stress. Young's modulus was assumed to be 2.0×10^5 MPa, and Poisson's ratio was taken as 0.3. The von-Mises yield criterion was applied for the material plasticity theory. The stress-strain relation of the material was assumed to be a tri-linear curve to account for stress-strain relations of the high strength performance steel, as shown in fig 4. The differences in FE results obtained with bi-linear and tri-linear model are shown in Figs. 5(a) and (b). Quite a similar structural behavior was traced up to peak load. However, some different strain-softening behavior was shown after peak load.

To investigate the effect of local and overall buckling interaction on the column strength, a linear elastic buckling analysis was first carried out to determine the initial imperfections in local buckling mode. Since the buckling interaction might be very sensitive to initial imperfections, the sensitivity to the magnitude of imperfections was examined. Figs. 6(a) and (b) show a comparison of the axial load versus displacement curves of the H sections obtained by the FE analysis. The curves were obtained with the various magnitudes of the initial imperfections. The initial imperfections in a local buckling mode were obtained with the magnification factors of 0.01h, 0.05h and 0.001h. A lateral triggering load was applied at the center of column to incur overall buckling interacted with local buckling. The maximum loads of the selected H section columns calculated with various magnitude imperfections in local buckling mode were similar, regardless of its magnitude and for both short and long columns. The magnitude of 0.001h for the initial imperfections was used in further analyses.

The effects of increasing the magnitude of the triggering load to impose the overall buckling mode in the minor axis

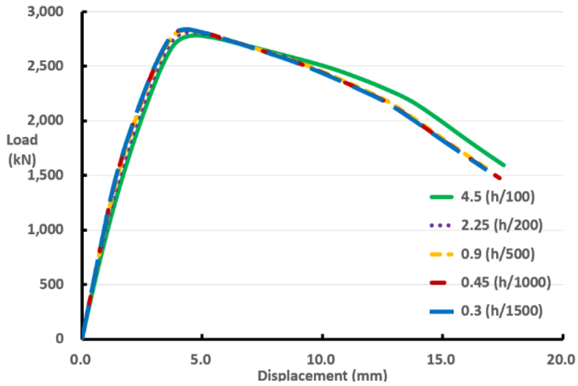

(a) H-450-240-7-7-1200

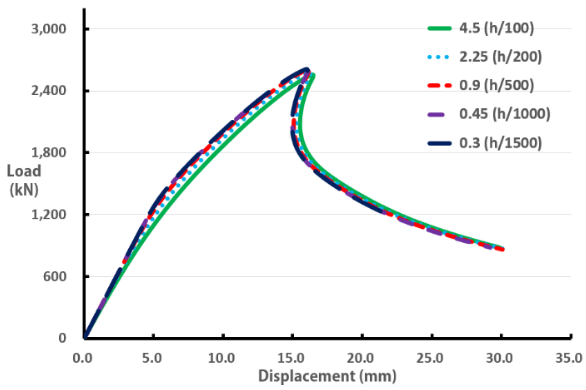

(b) H-450-240-7-7-5000

Fig. 6 Effects of initial imperfections in local buckling mode on the ultimate strength of column

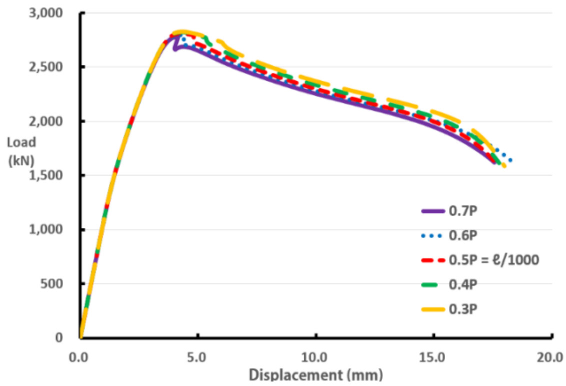

(a) 450-240-7-7-1200

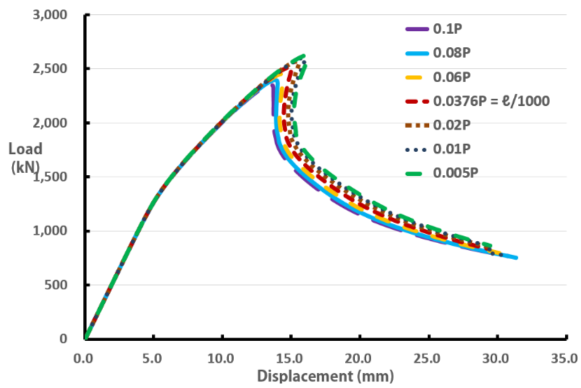

(b) H-450-240-7-7-5000

Fig. 7 Effects of triggering load for overall buckling on the ultimate strength of columns

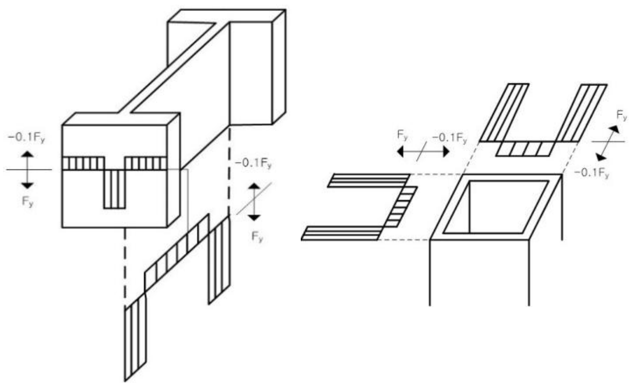

(a) Typical residual stress distribution model

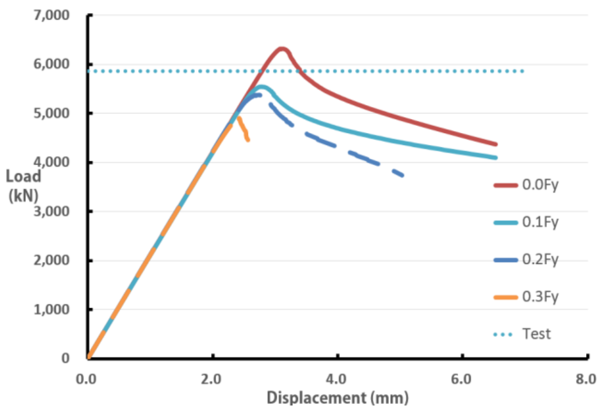

(b) Load versus displacement curve for H-249-240-12-9-5000 section column

Fig. 8 Effects of residual stress distribution on the ultimate strength of columns

direction were investigated. For the short column shown in Fig. 7(a), the effects of initial imperfections in the overall buckling mode on the structural behavior and the maximum load are negligible because the short column did not undergo overall buckling with a tiny triggering load. However, there are significant effects on the ultimate column strength for long columns, as shown in Fig. 7(b). The ultimate loads show significant differences between triggering loads of 0.1P to 0.02P, where the vertical reference load P is 93.0 kN. However, the ultimate load and the structural behavior show little differences between 0.005P, 0.02P, and 0.01P, as shown in Fig. 7(b). The magnitude L/1000 in overall buckling mode is equivalent to the triggering load 0.0376P. Based on these results, a triggering load of 0.01P was used for further analyses.

The effect of the magnitude of residual stress on the ultimate column strength was then investigated. The residual stress distribution of high strength steel have been investigated by many researchers (Kim *et al*. 2014, Wang *et al*. 2012, Jiang *et al*. 2017, Yang *et al*. 2016, Khan *et al*. 2016, Li *et al*. 2015, Zhang *et al*. 2016). Most researches including Rassmussen and Hancock (1992, 1995), and Kim *et al*. (2014) reported that the magnitude of the residual stress of the steel sections is independent of the yield stress. The magnitude of residual stress of high strength steel sections is comparatively smaller than that of mild steel. And therefore the effects of residual stress of high strength steel columns is less important than mild steel columns. However, the ideal pattern of magnitude of residual stress cannot be found. Kim *et al*. (2014) measured the residual stress for 800 MPa high performance steel sections produced in Korea.

The maximum value of membrane compressive residual stress was irregular and lower than -0.1F_y. The residual stress was included in the FE analysis as shown in Fig. 8(a), where the magnitude ranged from 0.0 to -0.3F_y for compression and +0.5F_y to +1.0F_y for tension. The resultant residual force should be in self-equilibrium across the section. The axial load versus displacement curves of the H-249-240-12-9-5000 section obtained by the LUSAS program with the various residual stress distributions are compared in Fig. 8(b). Measured Young's modulus of 196,210 MPa and yield stress of 761 MPa were used in the analysis. The difference in the maximum loads computed with various magnitudes from -0.3F_y to -0.0F_y for compression were not negligible. As the magnitude increased, the ultimate strength of the column was decreased. The FE result obtained without including residual stress is higher than the test result (Kim *et al*. 2014). The maximum loads computed with a magnitude 0.1F_y for compression was approximately 6% lower than the test ultimate load of the H-249-240-12-9-5000. Thus, this value has been used in subsequent FE analyses.

Table 1(a) Dimensions of H sections (Kim *et al*. 2014)

Specimens	F_y (MPa)	b_f (mm)	h (mm)	t_f (mm)	t_w (mm)	h/t_w	$b_f/2t_f$	L (mm)	A (mm^2)
H-310-220-15-15-900	760	220	310	15	15	18.7	8.2	900	11,400
H-380-220-15-15-1000	760	220	380	15	15	23.3	7.3	1000	12,450
H-450-240-15-15-1200	760	240	450	15	15	28.0	7.3	1200	13,500

Table 1(b) Dimensions of box sections (Im *et al*. 2005)

Specimens	F_y (MPa)	b_f (mm)	d (mm)	t_f (mm)	t_w (mm)	d/t_w	b/t_f	L (mm)	A (mm^2)
R-315-315-9-845	553	315	315	9	9	33.0	35.0	945	11,340
R-340-340-9-1020	553	340	340	9	9	35.8	37.8	1020	12,240
R-370-370-9-1110	553	370	370	9	9	39.1	41.1	1110	13,320

Table 2 Comparison of FE analysis, tests, current specifications

Specimens	Tests(kN)	FE(kN)	Tests/FE	EC3(kN)	Tests/EC3	FE/EC3
H-310-220-15-15-900	9,042	8,161	1.11	8,322	1.09	0.98
H-380-220-15-15-1000	9,244	8,650	1.07	9,120	1.01	0.95
H-450-240-15-15-1200	9,792	9,603	1.02	9,583	1.02	1.00
R-315-315-9-845	5,863	5,832	1.01	5,481	1.07	1.06
R-340-340-9-1020	5,947	5,875	1.01	5,617	1.06	1.05
R-370-370-9-1110	5,549	5,482	1.01	5,753	0.97	0.95
Average			1.04		1.04	1.00
S.D.			0.04		0.04	0.05

3.2 Verification of FE analysis results

The FE results were compared with test results from Kim *et al*. (2014) and Im *et al*. (2005). The dimensions of the test columns are summarized in Tables 1(a) and 1(b). The yield stresses of the test columns are 760 MPa for H sections and 553 MPa for Box sections. The results are compared in Table 2. The average ratio of measured ultimate strength to the FE result is 1.04, and the standard deviation is 0.004. The design strengths obtained by EC3 (European Committee for Standardisation 2003, 2006) are also included in Table 2 for verification of FE results. The average ratio of the FE results to these design strengths obtained by the EC3 is 1.0, and the standard deviation is 0.05. The comparison verifies that the FE results are quite reliable. Therefore, a parametric study was conducted with the same conditions to obtain an FE data base for high strength steel columns.

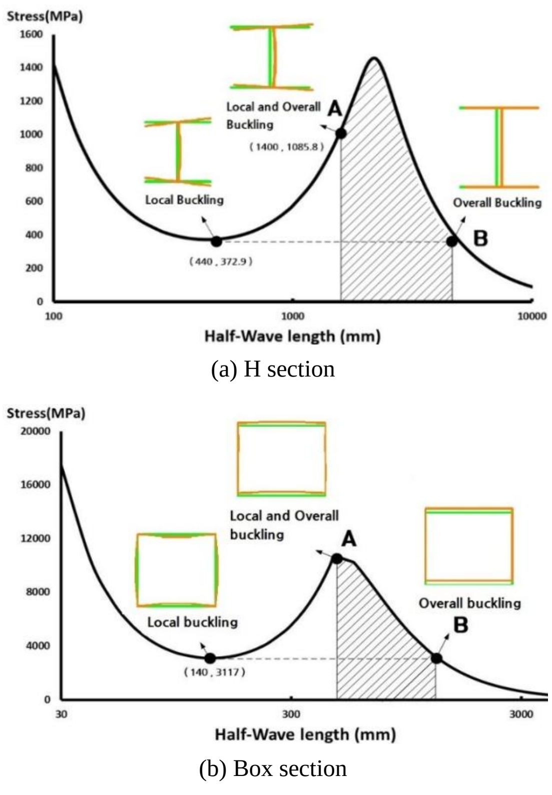

Fig. 9 Buckling stress versus half-wavelength curves

3.3 FE tests for high performance steel columns

3.3.1 Determination of section geometries for slender columns with buckling interaction

There is little research on the ultimate strength of high strength steel section columns undergoing local and post-local buckling before overall buckling and final failure. Thus, FE tests were conducted with focus on slender section columns. For columns composed of slender elements, the effect of post-local buckling on the column strength is an important point of the FE tests. To determine the adequate dimensions for FE test sections, the buckling stresses should be computed exactly. The elastic buckling stresses of H and Box specimens under uniform compression are shown in Figs. 9(a) and 9(b). The buckling stress versus half-wave length curves were obtained by using BAP software (Kwon 2000). The test column lengths should be determined so that a significant post-local buckling strength reserve may be displayed before overall buckling or material yielding.

The scheme for determining the overall column length is also illustrated in Figs. 9(a) and (b). The allowable specimen lengths of test for H sections are in the hatched area in Fig. 9(a). For the columns of the length between point A and B, overall buckling stress is not lower than local buckling stress. This helps to avoid failure due to only the local buckling without buckling interaction. To avoid the failure by the local buckling alone for the Box sections shown in Fig. 9(b), the overall length is determined to range from the maximum stress point A to point B, where the overall buckling stress is equal to the local buckling stress.

3.2.2 FE analysis results

The material and geometrical nonlinear analysis of FE test specimens was conducted using the program LUSAS with the FE model presented in Section 2. The geometric parameters b/t, h/t_w, and the overall column length were varied to produce a total of 80 columns. For the slender section columns, the local buckling slenderness $\lambda_l = \sqrt{(P_y/P_{crl})}$ is generally larger than 0.8, where P_{crl} (= $F_{crl}\times A$) is the elastic local buckling load, and P_y (= $F_y\times A$) is the yield load. The mixed buckling modes and the failure modes obtained by the FE analysis are illustrated in Figs. 10(a) and (b). The premature local buckling for slender sections deteriorates the overall column strength, but the post-local buckling strength reserve is significant and

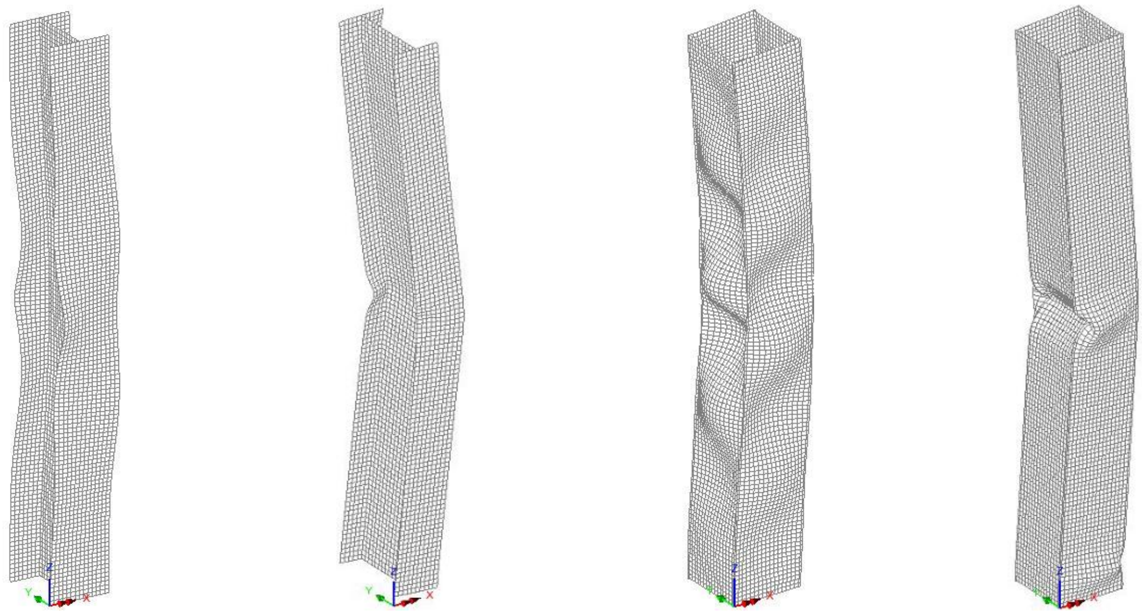

(a) H section (b) Box section

Fig. 10 Buckling and failure modes

Table 3(a) FE analysis results for H section columns

Specimens	$2b_f/t_f$	$h/_{tw}$	L (mm)	Elastic local buckling stress (Fcrl), MPa	Elastic local buckling load (Pcrl), kN	Maximum load (Pmax), kN	Yield load (Py), kN	(Pmax-Pcrl) /(Py-Pcrl)
H-320-180-10-10	9.0	30.0	1600	866	5,716	4,703	5,016	1.45
			1400	869	5,735	4,724		1.41
			1200	892	5,887	4,737		1.32
			1000	893	5,894	4,743		1.31
H-320-180-9-9	10.0	33.3	1600	698	4,146	3,930	4,514	-0.59
			1200	709	4,211	3,934		-0.91
			800	742	4,407	4,179		-2.14
H-320-180-8-8	11.3	37.5	2200	548	2,893	3,114	4,013	0.20
			1700	553	2,920	3,121		0.18
			1200	563	2,973	3,168		0.19
H-320-180-7-7	12.9	42.9	2400	420	1,940	2,356	3,511	0.26
			2000	423	1,954	2,406		0.29
			1600	426	1,968	2,428		0.30
			1200	433	2,000	2,440		0.29
H-450-220-10-10	11.0	43.0	7000	447	3,889	2,770	6,612	-0.41
			6000	450	3,915	3,738		-0.07
			5000	453	3,941	4,027		0.03
			4000	469	4,080	4,366		0.11
			3000	472	4,106	4,769		0.26
H-316-286-10-10	14.3	29.6	3400	583	5,060	5,102	6,597	0.03
			3000	584	5,069	5,104		0.02
			2600	587	5,095	5,363		0.18
			2000	594	5,156	5,421		0.18
H-316-286-9-9	15.9	33.1	4200	462	3,617	3,924	5,951	0.13
			3800	463	3,625	3,956		0.14

Table 3(a) Continued

Specimens	$2b_f/t_f$	$h/_{tw}$	L (mm)	Elastic local buckling stress (Fcrl), MPa	Elastic local buckling load (Pcrl), kN	Maximum load (Pmax), kN	Yield load (Py), kN	(Pmax-Pcrl) /(Py-Pcrl)
H-316-286-9-9	15.9	33.1	3200	463	3,625	3,981	5,951	0.15
			2600	468	3,664	4,047		0.17
			2000	470	3,680	4,143		0.20
H-316-286-8-8	17.9	37.5	4800	369	2,574	3,162	5,302	0.22
			4200	370	2,581	3,332		0.28
			3200	371	2,588	3,416		0.31
			2600	373	2,602	3,503		0.33
			2200	374	2,609	3,630		0.38
H-316-286-7-7	20.4	42.9	4200	278	1,701	2,702	4,650	0.34
			3200	284	1,738	2,796		0.37
			2600	285	1,744	2,840		0.39
H-414-380-7-7	27.1	57.1	9400	158	1,283	2,081	6,171	0.16
			8600	158	1,283	2,190		0.18
			7400	159	1,291	2,244		0.20
			5400	159	1,291	2,332		0.21
			4000	161	1,307	2,589		0.27
			3300	162	1,315	2,656		0.28
			2600	164	1,332	2,703		0.29
H-120-350-10-10	17.5	10.0	2800	502	4,016	4,560	6,080	0.26
			2400	504	4,032	4,600		0.28
			2000	521	4,176	4,615		0.23
			1600	522	4,432	4,671		0.15
			1000	554	4,760	4,706		-0.04
			800	595	4,760	4,777		0.01

Table 3(b) FE analysis results for Box section columns

Specimens	b_f/t_f	$h/_{tw}$	L (mm)	Elastic local buckling stress (Fcrl), MPa	Elastic local buckling load (Pcrl), kN	Maximum load (Pmax), kN	Yield load (Py), kN	(Pmax-Pcrl) /(Py-Pcrl)
R-320-320-10	32	30	5,000	732	9,367	8,284	9,728	-3.00
			4,000	732	9,364	8,323		-2.87
			3,000	734	9,396	8,377		-3.07
			2,000	735	9,402	8,396		-3.09
R-320-320-9	36	34	4,200	617	7,110	6,706	8,755	-0.25
			3,600	617	7,111	6,739		-0.23
			3,000	618	7,114	6,746		-0.22
			2,400	618	7,122	6,777		-0.21
			1,800	621	7,156	6,812		-0.22
R-320-320-8	40	38	6,000	490	5,016	4,998	7,782	-0.01
			5,000	490	5,022	5,090		0.02
			3,000	493	5,048	5,290		0.09
			2,500	495	5,070	5,299		0.08
R-320-320-10	32	30	5,000	732	9,367	8,284	9,728	-3.00
			4,000	732	9,364	8,323		-2.87

Table 3(b) Continued

Specimens	b_f/t_f	$h/_{tw}$	L (mm)	Elastic local buckling stress (Fcrl), MPa	Elastic local buckling load (Pcrl), kN	Maximum load (Pmax), kN	Yield load (Py), kN	(Pmax-Pcrl) /(Py-Pcrl)
R-320-320-10	32	30	3,000	734	9,396	8,377	9,728	-3.07
			2,000	735	9,402	8,396		-3.09
R-320-320-9	36	34	4,200	617	7,110	6,706	8,755	-0.25
			3,600	617	7,111	6,739		-0.23
			3,000	618	7,114	6,746		-0.22
			2,400	618	7,122	6,777		-0.21
			1,800	621	7,156	6,812		-0.22
R-320-320-8	40	38	6,000	490	5,016	4,998	7,782	-0.01
			5,000	490	5,022	5,090		0.02
			3,000	493	5,048	5,290		0.09
			2,500	495	5,070	5,299		0.08
R-320-320-7	46	44	6,000	379	3,398	3,932	6,810	0.16
			5,000	379	3,399	4,017		0.18
			4,000	380	3,401	4,023		0.18
			3,000	380	3,407	4,032		0.18
			1,800	382	3,419	4,121		0.21
R-270-260-8	34	31	3,000	719	6,100	5,063	6,455	-3.01
			2,500	721	6,117	5,192		-2.83
			2,000	724	6,139	5,228		-2.98
			1,500	726	6,152	5,271		-3.01
R-270-260-7	39	35	6,000	553	4,100	3,712	5,639	-0.25
			5,000	553	4,101	3,798		-0.20
			4,000	554	4,108	3,901		-0.14
			3,000	568	4,215	3,911		-0.21
			1,500	568	4,215	3,915		-0.21
R-270-260-6	45	41	3,000	402	2,557	2,923	4,834	0.16
			2,500	418	2,656	2,950		0.13
			2,000	420	2,674	2,989		0.15
R-420-320-8	53	38	5500	325	3,848	5,226	8,998	0.27
			4500	326	3,857	5,256		0.27
			3500	326	3,861	5,286		0.28
			2600	328	3,884	5,334		0.28
R-420-320-7	60	44	5500	245	2,538	4,006	7,844	0.28
			4500	249	2,580	4,092		0.29
			3500	250	2,590	4,144		0.29
			2600	253	2,621	4,156		0.29
R-420-320-6	70	51	5500	183	1,625	3,061	6,749	0.28
			4500	187	1,660	3,140		0.29
			3500	187	1,661	3,176		0.30
			2600	188	1,669	3,198		0.30

should therefore be accounted for in predicting the design strength of slender section columns.

FE results for the sections where the width-to-thickness of flanges ranges from 9.0 to 27.1 and that of web ranges from 10.0 to 57.1 are summarized in Tables 3(a) and 3(b). Elastic local buckling load is included in the tables for comparison. The post-buckling strength is estimated simply as $P_{max} - P_{crl}$ and is also included in the tables. As the width-to-thickness decreases, the post-buckling strength becomes increases. Negative values of $(P_{max} - P_{crl}) / (P_y - P_{crl})$ in the last column of the tables indicates that the elastic local buckling stress is larger than the maximum stress obtained by LUSAS, an inelastic local buckling is likely to occur, or the maximum load will decrease due to interaction between local and overall buckling. The larger elastic local buckling load than the yield load for the section H-320-180-10-10 means that the section yields instead of undergoing local buckling.

4. Direct strength formulae for high strength steel section columns

DSM incorporates empirical strength formulae based on test results and an elastic local buckling stress obtained through rigorous buckling analysis or theoretical equations if available. Therefore, the strength formulae developed on the basis of test results for mild steel members should be calibrated using results for high high-performance and high strength steel members. A set of compressive strength equations was developed recently for welded section columns based on test results for welded mild steel H and C section columns (Kwon *et al*. 2007)

for $\lambda_l \leq 0.816$

$$P_{\mathrm{nl}} = P_{ne} \tag{1a}$$

for $\lambda_l > 0.816$

$$P_{\mathrm{nl}} = \left[1 - 0.15\left(\frac{P_{crl}}{P_{ne}}\right)^{0.5}\right]\left(\frac{P_{crl}}{P_{ne}}\right)^{0.5} P_{ne} \tag{1b}$$

where

$$\lambda_{\mathrm{l}} = \sqrt{P_{ne}/P_{crl}} \tag{1c}$$

P_{nl} is the limiting load that accounts for local and overall buckling, P_{crl} $(=F_{crl} \times A)$ is the elastic local buckling load, and P_{ne} is the overall column strength based on the overall failure mode determined from the minimum of elastic flexural, torsional, and flexural-torsional buckling stresses. The overall column strength P_{ne} can be calculated using Eqs. (E3-2) and (E3-3) of the AISC specifications (2016), Eqs. (6.41) and (6.42) in Eurocode 3 (2003), or Eqs. (5.3-2) and (5.3-3) of the KISC specifications (2009) without accounting for local instability.

Design strength Eqs. (1a) and (1b) for the DSM are compared with FE results in Fig. 11, where the nominal column strength P_{ne} is based on EC3 and AISC specifications. Eqs. (1a) and (1b) agree well with the FE results for the H section columns, so it can be concluded that these equations can be used for the design strength curves for high strength steel welded H section columns. However, they are slightly unconservative for Box section columns, so the equations need modification for this case. In previous test results for mild steel welded Box sections (Kwon and Seo 2013), a slightly different set of compressive strength equations was proposed for welded Box section columns to account for the different structural

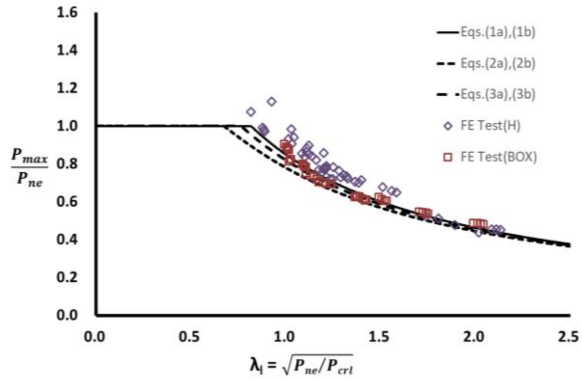

(a) Based on AISC specifications

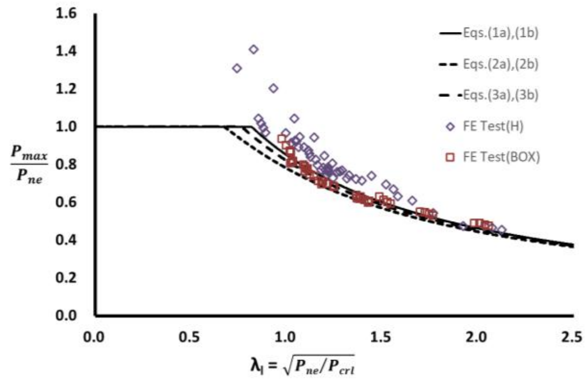

(b) Based on EC3

Fig. 11 Comparison of Eqs. (1a) and (1b) with FE results for H and Box section columns

characteristics from H sections. However, the strength predictions are too conservative for high local buckling slenderness.

To further validate Eqs. (1a) and (1b), they were compared with FE results and test results for welded high strength steel H section columns from the literature (Ban *et al*. 2012, Li *et al*. 2016, Kim *et al*. 2014, Rasmussen and Hancock 1989, Im *et al*. 2001, Shi *et al*. 2012). Test results of medium-high strength and mild steel sections are also included in the figures for comparison (Davids and Hancock 1986, Kwon *et al*. 2007, Kim *et al*. 2015, Im *et al*. 2001, 2005, Lee *et al*. 2015). Measured yield stresses of most medium-high strength steel sections tested were higher than the nominal yield stress of high strength steel (460 MPa). The results are shown in Figs. 12(a) and (b), where the nominal column strength P_{ne} is based on the AISC specifications or EC3. A few test results for welded C-section columns (Rasmussen and Hancock 1989) are also included in the figures for comparison. The strength predictions by Eqs. (1a) and (1b) are reasonably conservative for the high strength steel H section columns. However, the predictions are slightly unconservative for C section columns in comparison with the test results. The strength equations based on the AISC column strength curve predict slightly higher strength than those based on EC3 column curves. This results from the slightly different column strengths between the AISC specifications and EC3.

Kwon and Seo (2013) and Shen (2014) proposed direct strength formula for welded steel Box section columns.

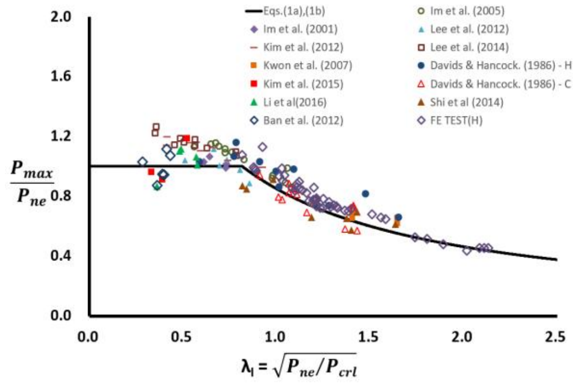

(a) Based on AISC column strength

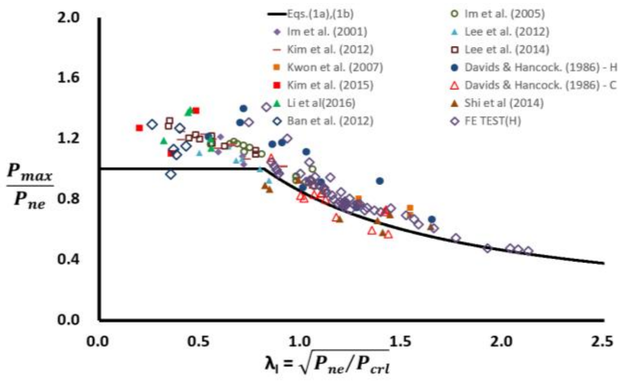

(b) Based on EC3 column strength

Fig. 12 Comparison of DSM and test results for welded H sections

They modified the coefficient or exponent from original Winter formula (1947). However, the strength predictions by those proposed formulae become slightly more or less conservative as the local buckling slenderness increases beyond 1.0. Winter formula can be taken as strength formulae for the DSM for high strength steel welded Box section columns. It has been adopted by ECS (2006) for the effective width equation for an internal compression element

for $\lambda \leq 0.673$

$$\frac{b_e}{b} = 1.0 \tag{2a}$$

for $\lambda > 0.673$

$$\frac{b_e}{b} = \frac{\lambda - 0.22}{\lambda^2} = \left[1 - 0.22\left(\frac{F_{crl}}{F_y}\right)^{0.5}\right]\left(\frac{F_{crl}}{F_y}\right)^{0.5} \leq 1.0 \tag{2b}$$

where

$$\lambda = \sqrt{\frac{F_y}{F_{crl}}} = \frac{b/t}{56.8\sqrt{235/F_y}} \tag{2c}$$

Eqs. (2a) and (2b) are included in Fig. 11 for direct comparison. The results for these equations lie below those of Eqs. (1a) and (1b) and reach them in the buckling range of the sections.

In order to provide a lower bound of high performance and high strength steel welded Box section columns, a modified set of strength equations can be given by

for $\lambda_l \leq 0.723$

$$P_{\rm nl} = P_{ne} \tag{3a}$$

for $\lambda_l > 0.723$

$$P_{\rm nl} = \left[1 - 0.2\left(\frac{P_{crl}}{P_{ne}}\right)^{0.5}\right]\left(\frac{P_{crl}}{P_{ne}}\right)^{0.5} P_{ne} \tag{3b}$$

where

$$\lambda_{\rm l} = \sqrt{P_{ne}/P_{crl}} \tag{3c}$$

Eq. (3b) is obtained by decreasing the coefficient of 0.22 in Eq. (2b) to 0.2 to provide a reasonable fit to the FE results for Box section columns in the range of large local buckling slenderness. The results for Eqs. (3a) and (3b) shown in Fig. 11 agree well with FE results for welded steel Box section columns.

The design strength Eqs. (3a) and (3b) for DSM are compared with FE results and test results for medium and

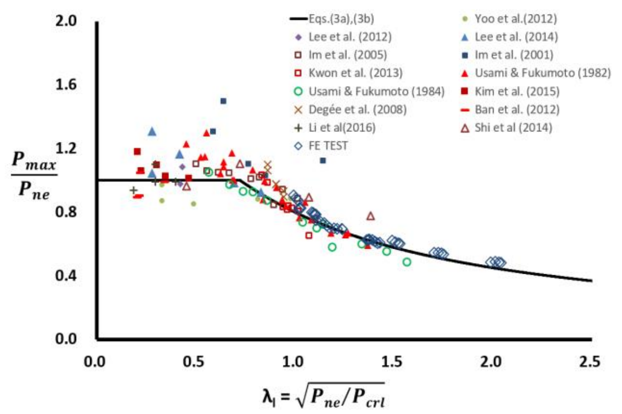

(a) Based on AISC column strength

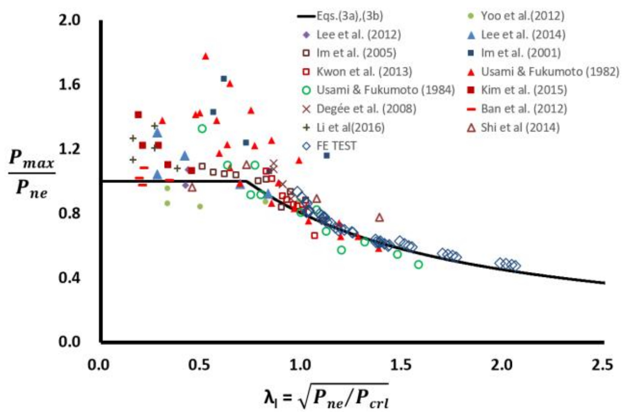

(b) Based on EC3 column strength

Fig. 13 Comparison of DSM and test results for welded Box sections

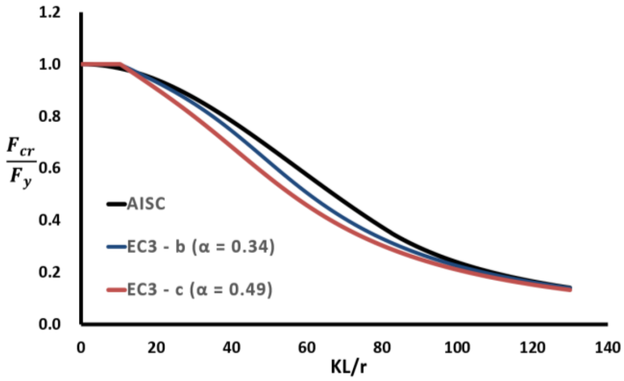

Fig. 14 Comparison of column strength curves for EC3 and AISC specifications

high strength steel Box section columns (Usami and Fukumoto 1982, 1984, Ban *et al*. 2012, Li *et al*. 2016, Degée *et al*. 2008, Kwon and Seo 2013, Kim *et al*. 2015, Im *et al*. 2001, 2005, Lee *et al*. 2015, Yoo *et al*. 2012, Shi *et al*. 2014) in Figs. 13(a) and (b). The results show that the equations can be used to predict quite reasonable strengths for high strength steel Box section columns as well as mild steel welded Box section columns. However, for the very slender sections tested by Usami and Fukumoto (1984), the predictions obtained by Eqs. (3a) and (3b) show a slight discrepancy. The DSM strength equations based on the EC3 in Fig. 13(b) produce slightly lower strengths than those based on the AISC specifications in Fig. 13(a). Figs. 12 and 13 show that Eqs. (1a) and (1b) can be directly used for H section columns with any strength grade where the nominal

Table 4 Comparison of tests, DSM, EC3, and AISC specifications for H sections

Specimens	Yield stress (MPa)	Specimens ($d \times b_f \times t_w \times t_f$)	Tests/ DSM-EC3	Tests/ DSM-AISC	EC3/ DSM-EC3	AISC/ DSM-EC3
Kim *et al*. (2014)	690 (815)	220x220x15x15	1.38	1.19	1.00	1.17
		150x150x15x15	1.66	1.31	1.00	1.27
		110x110x15x15	1.88	1.46	1.00	1.28
Lee *et al*. (2015)	440 (538)	159x96x9x12	1.28	1.22	1.00	1.01
		159x144x9x12	1.32	1.26	1.00	1.01
		159x192x9x12	1.22	1.18	1.00	1.00
		204x96x9x12	1.21	1.15	1.00	1.02
		204x144x9x12	1.23	1.19	1.00	1.00
		204x192x9x12	1.20	1.16	1.00	0.99
		204x240x9x12	1.10	1.07	1.00	0.99
		249x144x9x12	1.17	1.14	1.00	0.99
		249x192x9x12	1.15	1.12	1.00	0.99
		249x240x9x12	1.12	1.10	1.00	0.99
Kim *et al*. (2015)	325 (428)	370x200x15x15	1.03	0.98	1.00	1.06
		500x260x15x15	0.86	0.84	1.00	1.05
		630x320x15x15	0.75	0.74	0.90	1.00
Lee *et al*. (2012)	750 (760)	310x220x15x15	1.43	1.22	1.00	1.03
		380x220x15x15	1.01	1.26	1.00	1.02
		450x240x15x15	0.83	1.18	1.00	0.98
Im *et al*. (2001)	420 (594)	400x400x12x16	1.06	1.04	0.97	1.01
		400x300x12x16	1.03	0.99	1.00	1.03
		400x200x12x16	1.21	1.07	1.00	1.14
		350x200x9x16	1.08	1.02	0.98	1.03
		300x200x9x16	1.11	1.03	1.00	1.08
Im *et al*. (2005)	440 (533)	385x300x12x19	1.00	1.13	0.86	0.89
		380x320x12x16	1.00	1.09	0.90	0.92
		300x300x12x16	1.00	1.15	0.86	0.87
		350x300x12x16	1.00	1.15	0.85	0.87
		380x300x12x16	1.00	1.13	0.86	0.88
		420x300x12x16	1.00	1.11	0.87	0.88
		450x300x12x16	1.00	1.09	0.86	0.88

* values in ( ) are measured yield stresses

Table 4 Continued

Specimens	Yield stress (MPa)	Specimens ($d \times b_f \times t_w \times t_f$)	Tests/ DSM-EC3	Tests/ DSM-AISC	EC3/ DSM-EC3	AISC/ DSM-EC3
Im *et al*. (2005)	440 (533)	500x300x12x16	1.00	1.05	0.87	0.90
		290x420x9x16	1.00	1.09	0.92	0.98
		320x420x9x12	1.00	1.08	0.93	0.96
		380x420x9x16	1.00	1.06	0.93	0.93
		290x280x9x9	1.00	1.22	0.84	0.88
		460x375x12x12	1.00	1.09	0.89	0.91
		500x375x12x12	1.00	1.08	0.90	0.92
Kim *et al*. (2012)	690 (761)	159x96x9x12	1.19	1.14	1.00	1.05
		159x144x9x12	1.25	1.20	1.00	1.04
		159x192x9x12	1.16	1.13	1.00	1.03
		204x96x9x12	1.23	1.16	1.00	1.06
		204x144x9x12	1.20	1.16	1.00	1.03
		204x192x9x12	1.13	1.10	1.00	1.03
		204x240x9x12	1.13	1.10	1.05	1.09
		249x144x9x12	1.16	1.13	1.00	1.02
		249x192x9x12	1.06	1.04	1.00	1.01
		249x240x9x12	1.12	1.10	1.05	1.08
Davids and Hancock (1986)	350 (407)	201x190x5.1x5.1	1.22	1.12	0.92	1.14
		200x190x5.1x5.1	1.30	1.06	0.93	1.22
		202x190x5.3x5.3	1.21	1.03	0.96	1.18
		252x240x5.3x5.3	1.35	1.24	0.95	1.15
		251x240x5.1x5.1	1.28	1.13	0.91	1.15
		253x240x5.3x5.3	1.40	1.16	0.91	1.12
		320x310x5.1x5.1	1.44	1.34	1.01	1.12
		321x310x5.3x5.3	1.17	1.04	0.98	1.13
		251x240x5.1x5.1	1.04	1.03	1.00	1.12
		251x240x5.1x5.1	1.08	1.07	1.01	1.10
		321x310x5.1x5.1	1.21	1.20	1.02	1.08
Kwon *et al*. (2007)	240 (350)	400x100x6x6	1.23	1.14	1.01	1.17
		550x160x6x6	1.34	1.26	1.20	1.27
		550x160x6x6	1.43	1.34	1.20	1.28
		500x140x6x6	1.24	1.14	1.11	1.21
		500x140x6x6	1.29	1.19	1.11	1.32
Li *et al*.(2016)	690 (772)	259x261x16.08x16.08	1.14	1.01	1.00	1.13
		260x261x16.08x16.08	1.20	1.06	1.00	1.13
		236x242x16.08x16.08	1.39	1.12	1.00	1.25
		238x242x16.08x16.08	1.38	1.10	1.00	1.25
		205x209x16.08x16.08	0.98	0.71	1.00	1.37
		205x209x16.08x16.08	1.19	0.87	1.00	1.37
Shi *et al*. (2014)	460 (493)	451x207x11.16x14.93	0.89	0.87	0.97	0.99
		632x290x10.67x15.05	1.08	1.07	1.18	1.18
		752x346x10.69x15.14	1.12	1.11	1.26	1.32
		279x350x12.88x13.04	0.89	0.87	0.88	1.06

* values in ( ) are measured yield stresses

Table 4 Continued

Specimens	Yield stress (MPa)	Specimens ($d \times b_f \times t_w \times t_f$)	Tests/ DSM-EC3	Tests/ DSM-AISC	EC3/ DSM-EC3	AISC/ DSM-EC3
Shi *et al*. (2014)	460 (493)	387x493x12.46x12.47	0.91	0.90	0.94	1.12
		459x589x12.75x12.53	0.91	0.90	0.95	1.11
		446x348x10.94x12.62	1.08	1.06	1.01	1.20
		625x491x11.11x12.6	1.02	1.01	1.04	1.23
		748x588x11.16x12.69	1.12	1.11	1.04	1.21
Ban *et al*. (2012)	460 (532)	208x210x15.02x14.80	1.15	1.07	1.00	1.07
		142x180x12.96x15.16	0.97	0.87	1.00	1.11
		150x152x11.35x11.08	1.10	0.94	1.00	1.16
		151x151x11.07x11.02	1.13	0.95	1.00	1.19
		111x132x11.34x10.76	1.29	1.03	1.00	1.26
		149x150x11.09x11.02	1.27	1.12	1.00	1.14
Total 85 sections		Average	1.09	1.07	0.99	1.04
		SD	0.20	0.11	0.08	0.23
		COV	0.04	0.01	0.01	0.05

* values in ( ) are measured yield stresses

Table 5 Comparison of tests, DSM, EC3, and AISC specifications for Box sections

Specimens	Yield stress (MPa)	Specimens ($d \times b \times t$)	Tests/ DSM-EC3	Tests/ DSM-AISC	EC3/ DSM-EC3	AISC/ DSM-EC3
Yoo *et al*. (2012)	690 (761)	90x90x9	0.96	0.97	1.00	0.99
		135x135x9	0.84	0.85	1.00	0.99
		180x180x9	0.86	0.87	1.00	0.99
		225x225x9	0.94	0.95	1.08	1.07
		270x270x9	1.08	1.09	1.09	1.11
Im *et al*. (2005)	440 (533)	225x225x12	1.09	1.10	1.00	0.99
		250x250x12	1.05	1.06	1.00	0.99
		275x275x12	1.04	1.05	1.00	0.99
		300x300x12	1.04	1.04	1.00	0.99
		350x350x12	1.05	1.06	1.05	1.05
		275x275x9	1.10	1.11	1.05	1.08
		300x300x9	0.97	0.97	1.04	1.10
		315x315x9	1.12	1.12	1.05	1.10
		340x340x9	1.11	1.12	1.05	1.10
		370x370x9	1.02	1.02	1.06	1.09
Im *et al*. (2001)	420 (594)	300x300x12	1.63	1.50	1.00	1.09
		275x275x12	1.43	1.31	1.00	1.09
		300x300x9	1.17	1.15	0.99	1.11
		400x400x9	1.58	1.56	1.03	1.11
		275x275x9	1.24	1.14	0.95	1.12
Kwon and Seo (2013)	315 (370)	250x230x6	1.15	1.13	1.36	1.11
		250x250x6	1.13	1.11	1.39	1.13
		300x180x6	1.05	0.99	1.47	1.14
		300x220x6	1.04	1.02	1.43	1.13
		300x270x6	1.03	1.02	1.47	1.12

* values in ( ) are measured yield stresses

Table 5 Continued

Specimens	Yield stress (MPa)	Specimens ($d \times b \times t$)	Tests/ DSM-EC3	Tests/ DSM-AISC	EC3/ DSM-EC3	AISC/ DSM-EC3
Kwon and Seo (2013)	315 (370)	310x160x6	1.04	0.99	1.48	1.13
		310x200x6	1.03	1.02	1.44	1.12
		310x290x6	0.87	0.86	1.51	1.12
Usami and Fukumoto (1982)	690 (741)	127x151x6	0.99	1.00	1.00	0.99
		156x181x6	0.96	0.97	1.03	1.06
		193x217x6	0.96	0.97	1.04	1.08
		223x246x6	0.94	0.95	1.05	1.08
		259x283x6	0.94	0.95	1.06	1.08
		127x151x6	1.18	1.04	1.00	1.13
		193x216x6	1.13	1.05	0.98	1.17
		223x247x6	1.07	1.00	1.01	1.17
		259x283x6	1.05	0.98	1.03	1.17
		122x151x6	1.42	1.15	1.00	1.24
		157x181x6	1.23	1.00	0.96	1.23
		192x217x6	1.27	1.11	0.93	1.23
		93.5x151x6	1.09	1.09	1.00	1.00
		144x217x6	1.01	1.01	1.05	1.07
		193x283x6	1.00	1.01	1.09	1.13
		94.2x151x6	1.42	1.14	1.00	1.24
		116x181x6	1.38	1.12	0.96	1.24
		144x217x6	1.47	1.12	1.04	1.33
		166x247x6	1.39	1.11	1.05	1.33
		193x283x6	1.40	1.12	1.11	1.40
		94.4x151x6	1.38	1.23	0.87	1.12
		116x181x6	1.78	1.30	1.03	1.37
		143x217x6	1.61	1.17	1.01	1.37
Usami and Fukumoto (1984)	460 (568)	216x147x4.5	0.97	0.98	1.00	1.03
		193x214x4.5	0.82	0.83	1.03	1.07
		256x276x4.5	0.87	0.88	1.05	1.07
		96x147x4.5	0.93	0.94	0.95	0.98
		143x214x4.5	0.94	0.95	1.07	1.11
		191x278x4.5	0.93	0.94	1.09	1.12
		93x147x4.5	1.10	0.97	0.95	1.13
		143x214x4.5	1.00	0.95	1.02	1.17
		191x277x4.5	0.96	0.94	1.08	1.15
		94x147x4.5	1.33	1.05	0.97	1.26
		143x214x4.5	1.14	0.98	0.93	1.21
		191x277x4.5	1.08	1.00	1.07	1.21
Kim *et al*. (2015)	325 (486)	240x240x15	1.07	1.01	1.00	1.05
		160x160x15	1.22	1.10	1.00	1.11
	690 (815)	240x240x15	1.41	1.18	1.00	1.20
		160x160x15	1.10	1.02	1.00	1.07
		120x120x15	1.22	1.06	1.00	1.15

* values in ( ) are measured yield stresses

Table 5 Continued

Specimens	Yield stress (MPa)	Specimens ($d \times b \times t$)	Tests/ DSM-EC3	Tests/ DSM-AISC	EC3/ DSM-EC3	AISC/ DSM-EC3
Lee *et al*. (2015)	440 (538)	90x90x9	0.96	1.31	1.00	1.00
		135x135x9	0.84	1.16	1.00	1.00
		180x180x9	0.86	1.04	1.00	1.00
		225x225x9	0.94	0.99	1.08	1.00
		270x270x9	1.08	1.01	1.09	1.09
Degée *et al*. (2008)	355 (390)	230x250x6	1.07	1.07	1.06	1.03
		230x250x6	1.11	1.12	1.06	1.03
		230x250x6	1.14	1.14	1.04	1.04
		230x250x6	1.14	1.13	1.04	1.04
		230x250x6	1.25	1.24	1.01	1.04
		230x250x6	1.21	1.20	1.01	1.04
Ban *et al*. (2012)	460 (532)	152x152x10.92	1.01	0.99	1.00	1.01
		141.1x141.1x14.83	1.08	1.05	1.00	1.04
		121.5x121.5x12.67	0.98	0.90	1.00	1.08
		102.4x102.4x11.04	1.02	0.89	1.00	1.14
Li *et al*. (2016)	690 (772)	236.23x236.23x16.2	1.08	0.99	1.00	1.09
		236.47x236.47x16.1	1.08	0.99	1.00	1.09
		192.37x192.37x16.02	1.21	0.99	1.00	1.22
		192.52x192.52x16.02	1.34	1.10	1.00	1.22
		140.88x140.88x16.07	1.27	0.94	1.00	1.35
		140.48x140.48x16.08	1.13	0.84	1.00	1.35
Shi *et al*. (2014)	460 (493)	236.23x236.23x12.72	0.96	0.96	1.00	1.00
		408.5x236.47x12.72	1.10	1.11	0.96	0.98
		500.9x192.37x10.69	1.18	1.18	1.03	1.04
		660.8x192.52x10.76	1.26	1.26	1.07	1.07
Total 93 sections		Average	1.12	1.05	1.05	1.11
		SD	0.19	0.13	0.13	0.10
		COV	0.03	0.02	0.02	0.01

* values in ( ) are measured yield stresses

yield stress ranges from 235 MPa to 690 MPa, while Eqs. (3a) and (3b) can be used for Box section columns with column strength based on AISC specifications or EC3.

To clarify the differences between predicted strengths obtained by the DSM based on the design column curve in EC3 and AISC specifications shown in Figs. 12(a), (b) and 13(a), (b), the column strength curves in the EC3 and AISC specifications are compared in Fig. 14. The estimated difference between the EC3 and AISC column strength curves is to be approximately 30% at a slenderness of around 60. The column strength in the AISC specifications is generally greater than that in EC3. The reduction factor for column strength is 0.9 in the AISC specifications, while the partial factor in EC3 is 1.1 for the resistance of members to column buckling and 1.0 for the strength of cross sections to material yielding including local buckling. Thus, the nominal column strengths can be compared directly. Therefore, designers can choose the column strength P_{ne} from the two basic column strength curves according to their preference, or they can also use the column strength curve provided in their national code.

5. Comparison of DSM, current specifications, and tests for welded section columns

Predicted column strengths obtained by the DSM based on EC3 (DSM-EC3) and AISC specifications (DSM-AISC) were compared with those calculated by EC3 and AISC specifications, and test results of various grade strength steel columns, as shown in Tables 4 and 5. The results from Eqs. (1a), (1b), (3a), and (3b) were normalized by DSM-EC3 for the comparison. The test yield stress rather than the nominal yield stress was used for the DSM prediction rather than the nominal yield stress. Generally, the measured yield stress is greater than the nominal yield stress for all the test results by approximately from 1.3 to 45.3%. The nominal and test yield stresses are also listed in the tables, and the values in parentheses are the measured yield stress.

For H section columns, the average ratio of the test results to the DSM-EC3 results is 1.09, and that for the DSM-AISC results is 1.07. The coefficient of variance of the test results to the DSM-EC3 results is 0.04, and that for the DSM-AISC results is 0.01. The average ratio of EC3 to DSM-EC3 is 0.99, and that of AISC to DSM-EC3 is 1.04 for H section columns. The predictions by the DSM based on the EC3 column strength lie between those obtained by the EC3 and AISC specifications. For Box section columns, the average ratio of the test results to the DSM-EC3 results is 1.12 and that for the DSM-AISC results is 1.05. The coefficient of variance of the test results to the DSM-EC3 results is 0.02, and that for DSM-AISC is also 0.02. The average ratio of EC3 to DSM-EC3 is 1.05, and that of AISC to DSM-EC3 is also 1.12 for box section columns.

The predicted safety margins are slightly different between H and box section columns, as shown in Tables 4 and 5. The average ratios of the column strength based on the AISC specifications to that based on the EC3 are approximately 1.01 for H sections and 1.07 for box sections. However, the proposed strength formulae for the DSM based on either the AISC column strength or EC3 column strength can predict reasonable strengths for high strength steel section columns. Therefore, the formulae for the DSM can be efficiently used to predict the nominal compressive strength for high strength steel welded section columns.

6. Conclusions

The direct strength method (DSM) is an advanced design method for thin-walled steel members and has been formally adopted for cold-formed steel members in North American specifications and Australian/New Zealand standards. The strength formulae for the DSM have been recently proposed to apply the method to the prediction of the ultimate strength for mild welded section structural members. However, the method has not been studied for high strength steel welded steel structural members yet. Since high performance and high strength steel sections have different mechanical characteristics from mild steel sections, the strength formulae for the DSM needed to be modified. Comparison of various test results and FE results with the proposed DSM predictions proved that the strength formulae can be used for the design of high strength steel welded section columns as well as mild steel sections. However, further researches should be conducted to apply the DSM to the practical design of high strength welded steel section columns. The detail design guide lines for the DSM based on the proposed strength formulae can be tentatively used as an alternative design method for high strength steel welded section columns in the AISC, KISC or other current design specifications before formal adoption as for cold-formed steel sections in the AISI specifications.

Acknowledgments

This research was supported by the 2017 Yeungnam University Research Grant, which was gratefully acknowledged.

References

Akrami, V. and Erfani, S. (2015), “Effect of local web buckling on the behavior of reduced web beam section”, *Steel Compos. Struct., Int. J.*, **18**(3), 641-657.

American Institute of Steel Construction (AISC) (2016), Design Specification for Steel Structural Buildings; Chicago, Il, USA.

American Iron and Steel Institute (AISI) (2004), Supplement 2004 to the North American Specifications for the Design of Cold-Formed Steel Structural Members; Washington DC, USA.

Ban, H., Shi, G., Shi, Y. and Wang, Y. (2012), “Overall buckling behavior of 460 MPa high strength steel columns: Experimental investigation and design method”, *J. Constr. Steel Res.*, **74**, 140-150.

Davids, A.J. and Hancock, G.J. (1986), “Compression tests of long welded I-section columns”, *J. Struct. Eng., ASCE*, **112**(10), 2281-2297.

Degée, H., Detzel, A. and Kuhlmann, U. (2008), “Interaction of global and local buckling in welded RHS compression members”, *J. Constr. Steel Res.*, **64**, 755-765.

European Committee for Standardisation (ECS) (2003), Eurocode 3: Design of Steel Structures; Brussels, Belgium.

European Committee for Standardisation (ECS) (2006), Eurocode 3: Design of Steel Structures, Part 1-5: Plated Structural Elements; Brussels, Belgium.

FEA Co., Ltd. (2012), LUSAS Element Reference Manual & User’s Manual (version 14.7); London, UK.

Gao, L., Sun, H., Jin, F. and Fan, H. (2009), “Load-carrying capacity of high-strength steel box-sections I: Stub columns”, *J. Constr. Steel Res.*, **65**, 918-924.

Gheidi, A., Mirtaheri, M., Zandi, A.P. and Alanjari, P. (2011), “Effect of filler material on local and global behavior of buckling-restrained braces”, *Struct. Des. Tall Special Build.*, **20**(6), 700-710.

Im, S.W., Ko, S.K. and Chang, I.H. (2001), “A study on the characteristics of high strength steel (SM570) plates in compression members”, *J. Korean Soc. Steel Constr., KSSC*, **13**(3), 222-232. [In Korean]

Im, S.W., Kim, Y.S. and Chang, I.H. (2005), “A study on the characteristics of SM570TMC plates in compression members”, *J. Korean Soc. Steel Const.*, KSSC, **17**(3), 357-363. [In Korean]

Jiang, J., Chiew, S.P., Lee, C.K. and Tiong, P.L.Y. (2017), “An experimental study on residual stresses of high strength steel box columns”, *J. Constr. Steel Res.*, **130**, 12-21.

Kenyon, D., Shu, Y., Fan, X., Reddy, S. and Lew, A.J. (2018), “Parametric design of multi-cell thin-walled structures for improved crashworthiness with stable progressive buckling mode”, *Thin-Wall. Sruct.*, **131**, 76-87.

Khan, M., Paradowska, A., Uy, B., Mashiri, F. and Tao, Z. (2016), “Residual stresses in high strength steel welded box sections”, *J. Constr. Steel Res.*, **116**, 55-64.

Kim, T.S., Lee, M.J., Oh, Y.S., Lee, K.M. and Kim, D.H. (2012), “A study on compressive strength of built-up H shaped columns fabricated with HSA800 high performance steels”, *J. Korean Soc. Steel Constr., KSSC*, **24**(6), 627-636. [In Korean]

Kim, D.K., Lee, C.H., Han, K.H., Kim, J.H., Lee, S.E. and Sim, H.B. (2014), “Strength and residual stress evaluation of stub columns fabricated from 800 MPa high strength steel”, *J. Constr. Steel Res.*, **102**, 111-120.

Kim, D.K., Lee, C.H., Han, K.H., Kim, J.H., Lee, S.E. and Kim, J.W. (2015), "Buckling Strength of Concentrically Loaded High-Strength Steel Columns with Intermediate Slenderness", *J. Korean Soc. Steel Constr., KSSC*, **27**(4), 377-386. [In Korean]

Korean Institute of Steel Construction (KISC) (2009), Design Specifications for Steel Structures-Load and Resistance Factor Design, Department of Land and Transportation, Seoul, Korea.

Kwon, Y.B. (2000), Buckling Analysis Program (BAP) User's Manual (version 2.0); Department of Civil Engineering, Yeungnam University, Gyeongsan, Korea.

Kwon, Y.B. (2014), "Development of direct strength method for welded section members", *Thin-Wall. Struct.*, **81**, 121-131.

Kwon, Y.B. and Seo, E.G. (2013), "Prediction of the compressive strength of welded RHS columns undergoing buckling interaction", *Thin-Wall. Struct.*, **68**, 141-55.

Kwon, Y.B., Kim, N.G. and Hancock, G.J. (2007), "Compression Tests of Welded Section Columns Undergoing Buckling Interaction", *J. Constr. Steel Res.*, **63**, 1590-1602.

Lee, K.M., Lee, M.J., Oh, Y.S. and Kim, T.S. (2012), "Local buckling behavior of stub H-shaped columns fabricated with HSA800 high performance steels under concentric loading", *J. Korean Soc. Steel Constr., KSSC*, **25**(3), 289-297. [In Korean]

Lee, K.M., Lee, M.J., Oh, Y.S., Yang, Y. and Oh, K.Y. (2015), "A comparative study on stub columns with various steel grades subjected to concentric axial loading", *Int. J. Steel Struct., KSSC*, **15**(1), 103-114.

Li, T.J., Li, G.Q. and Wang, Y.B. (2015), "Residual stress tests of welded Q690 high strength steel box and H-sections", *J. Constr. Steel Res.*, **115**, 283-289.

Li, T.J., Li, G.Q., Chan, S.L. and Wang, Y.B. (2016), "Behavior of Q690 high-strength steel columns: Part 1: Experimental", *J. Constr. Steel Res.*, **123**, 18-30.

Martins, A.D., Dinis, P.B. and Camotim, D. (2016), "On the influence of local-distortional interaction in behavior and design of cold-formed steel web stiffened lipped channel columns", *Thin-Wall. Struct.*, **101**, 181-204.

Mirtaheri, S.M. and Zoghi, M.A. (2016), "Design guides to resist progressive collapse of steel structures", *Steel Compos. Struct., Int. J.*, **20**(2), 357-378.

Mirtaheri, S.M., Nazeryan, M., Bahrani, K.M., Nooralizadeh, A., Montazerian, L. and Naserifard, M. (2017), "Local and global buckling condition of all-steel buckling restrained braces", *Steel Compos. Struct., Int. J.*, **23**(2), 217-228.

Miyachi, K., Nakamura, S. and Manda, A. (2012), "Progressive collapse analysis of steel truss bridges and evaluation of ductility", *J. Constr. Steel Res.*, **78**, 192-200.

Paik, J.K. and Kim, B.J. (2008), "Progressive collapse analysis of thin-walled box columns", *Thin-Wall. Struct.*, **46**, 541-550.

Park, J.W. and Yoo, J.H. (2013), "Axial load tests and load capacity of slender SHS stub columns strengthened with carbon fiber reinforced polymers", *Steel Compos. Struct., Int. J.*, **15**(2), 131-150.

Pham, C.H. and Hancock, G.J. (2012), "Elastic buckling of cold-formed channel sections in shear", *Thin-Wall. Struct.*, **61**, 22-26.

Rasmussen, K.J.R. and Hancock, G.J. (1989), "Compression tests of welded channel section columns", *J. Struct. Eng., ASCE*, **115**(4), 789-808.

Rasmussen, K.J.R. and Hancock, G.J. (1992), "Plate slenderness limits for high strength steel sections", *J. Constr. Steel Res.*, **23**, 73-96.

Rasmussen, K.J.R. and Hancock, G.J. (1995), "Tests of high strength steel columns", *J. Constr. Steel Res.*, **34**, 27-52.

Schafer, B.W. and Pekoz, T. (1998), "Direct strength prediction of cold-formed steel members using numerical elastic buckling solutions", *Thin-Wall. Struct., Res. Develop.*, (Eds. by N.E. Shanmugan, J.Y.R. Liew and V. Thevendran), Elsevier, pp. 137-144.

Shen, H. (2014), "On the direct strength and effective yield strength method design of medium and high strength steel welded square section columns with slender plate elements", *Steel Compos. Struct., Int. J.*, **17**(4), 497-516.

Shi, G., Ban, H. and Bijlaard, F.S.K. (2012), "Tests of numerical study of ultra-high strength steel columns with end restraints", *J. Constr. Steel Res.*, **70**, 236-247.

Shi, G., Zhou, W., Bai, Y. and Lin, C. (2014), "Local buckling of 460 MPa high strength steel welded section stub columns under axial compression", *J. Constr. Steel Res.*, **100**, 60-70.

Standard Australia (2005), Cold-Formed Steel Structures AS/NZS 4600; Sydney, NSW, Australia.

Usami, T. and Fukumoto, Y. (1982), "Local and Overall Buckling of Welded Box Columns", *J. Struct. Eng., ASCE*, **108**(ST3), 525-542.

Usami, T. and Fukumoto, Y. (1984), "Welded Box Column Members", *J. Struct. Eng., ASCE*, **110**(10), 2457-2470.

Wang, Y.B., Li, G.Q. and Chen, S.W. (2012), "Residual Stresses in Welded Flame-cut High strength Steel H-Sections", *J. Constr. Steel Res.*, **79**, 159-165.

Winter, G. (1947), "Strength of thin steel compression flanges", *Transactions, ASCE*, **112**(2305), 527-576.

Yang, B., Nie, S., Xiong, G., Hu, Y., Bai, J., Zhang,W. and Dai, G. (2016), "Residual stresses in welded I-shaped sections fabricated from Q460GJ structural steel plates", *J. Constr. Steel Res.*, **122**, 261-273.

Yoo, J.H., Kim, J.W., Yang, J.K., Kang, J.W. and Lee, D.W. (2012), " Local buckling of built-up square tubular compression members fabricated with HSA800 high performance steels under concentric axial loading", *J. Korean Soc. Steel Constr., KSSC*, **24**(4), 435-442. [In Korean]

Young, B., Silvestre, N. and Camotim, D. (2013), "Cold-formed steel lipped channel columns influenced by local-distortional interaction; strength and DSM design", *J. Struct. Eng., ASCE*, **139**(6), 1059-1074.

Zhang, X., Zhao, M. and Chiew, S.P. (2016), "Residual stress of cold-formed thick-walled steel rectangular hollow sections", *Steel Compos. Struct., Int. J.*, **20**(4), 837-853.

CC